Propensity for the Air/Water Interface and Ion Pairing in Magnesium Acetate vs Magnesium Nitrate Solutions: Molecular Dynamics Simulations and Surface Tension Measurements

Babak Minofar,[†] Robert Vácha,[†] Abdul Wahab,[‡] Sekh Mahiuddin,[‡] Werner Kunz,[§] and Pavel Jungwirth*,[†]

Institute of Organic Chemistry and Biochemistry, Academy of Sciences of the Czech Republic, and Center for Biomolecules and Complex Molecular Systems, Flemingovo nám. 2, 16610 Prague 6, Czech Republic, Material Science Division, Regional Research Laboratory, Jorhat-785 006, Assam, India, and Institut für Physikalische und Theoretische Chemie, Universität Regensburg, D-93040 Regensburg, Germany

Received: January 30, 2006; In Final Form: June 13, 2006

Molecular dynamics simulations in slab geometry and surface tension measurements were performed for aqueous solutions of magnesium acetate and magnesium nitrate at various concentrations. The simulations reveal a strong affinity of acetate anions for the surface, while nitrate exhibits only a very weak surface propensity, and magnesium is per se strongly repelled from the air/water interface. CH_3COO^- also exhibits a much stronger tendency than NO_3^- for ion pairing with Mg^{2+} in the bulk and particularly in the interfacial layer. The different interfacial behavior of the two anions is reflected by the opposite concentration dependence (beyond 0.5 M) of surface tension of the corresponding magnesium salts. Measurements, supported by simulations, show that the surface tension of $Mg(NO_3)_2$(aq) increases with concentration as for other inorganic salts. However, in the case of $Mg(OAc)_2$(aq) the surface tension isotherm exhibits a turnover around 0.5 M, after which it starts to decrease, indicating a positive net solute excess in the interfacial layer at higher concentrations.

Introduction

Ion pairing is an important manifestation of nonideal behavior of aqueous electrolyte solutions at finite concentrations.[1] In the higher concentration region (particularly close to the solubility limit) ion pairing is prevalent for all salts; however, at lower concentrations the tendency of monovalent inorganic ions for pairing is relatively weak.[2−8] Ion pairing is stronger in solutions of polyvalent ions[9,10] or for salts in which one ion is multiply charged,[11,12] particularly if the other ion exhibits a certain degree of hydrophobicity, such as small organic ions.[13,14]

The process of ion pairing is usually investigated in the bulk of the electrolyte solution. New interesting questions, however, arise in anisotropic regions of the solution, such as the interface between the aqueous solution and a medium with a low dielectric constant. Most recently, the issue ion pairing at a hydrophobic surface, which can have important biological and technological implications, has been addressed.[15] Molecular dynamics simulations (MD) showed that the presence of a model surface could strongly influence the tendency of aqueous ions to form pairs.[15]

Conceptually, the simplest of such surfaces is the interface between water and vapor or air. This interface is traditionally viewed as devoid of simple ions due to image charge repulsion.[16,17] However, recent molecular dynamics simulations,[18−22] as well as surface selective experiments,[23−26] indicate that polarizable inorganic ions, such as heavier halides, exhibit a significant propensity for the aqueous surface. Moreover, small organic ions, containing a methyl group or a short aliphatic chain can be naturally driven to the surface due to the hydrophobicity of these groups.

In our previous study, we investigated experimentally and computationally bulk properties, including ion pair formation of aqueous magnesium acetate and nitrate.[14] We found a strong tendency for ion pairing in the former system and a lack of it in the latter one, which allowed us to rationalize differences in bulk properties such as electrical conductivities of the two solutions. In this work we focus on the air/solution interface of $Mg(OAc)_2$(aq) and $Mg(NO_3)_3$(aq), which we characterize by means of MD simulations and surface tension measurements. We point out the strikingly different interfacial structure of the two solutions, which we trace back to different hydration properties of the corresponding anions.

Systems and Computational Method

Classical molecular dynamics simulations of solutions of magnesium nitrate and magnesium acetate were performed in a slab geometry.[27,28] The unit cell contained 863 water molecules; 8, 16, or 32 magnesium cations; and 16, 32, or 64 anions (nitrate or acetate), which corresponds roughly to 0.5, 1, or 2 M salt concentrations. The size of the prismatic unit cell was approximately 30 × 30 × 100 Å, and 3D periodic boundary conditions were applied.[29] Due to the finite size of the unit cell with a fixed total number of ions therein and due to generally different amounts of ions in the bulk and interfacial regions, the actual bulk concentrations can differ significantly from the nominal values given above. This is particularly true for cases of strong surface ion enhancement, which leaves the bulk region significantly depleted of ions.

* Corresponding author. E-mail: pavel.jungwirth@uochb.cas.cz.
[†] Academy of Sciences of the Czech Republic.
[‡] Regional Research Laboratory.
[§] Universität Regensburg.

10.1021/jp060627p CCC: $33.50
Published on Web 07/25/2006

TABLE 1: Charges (*e*), Polarizabilities (α, in Å^3), and Lennard-Jones Parameters in Amber Convention (R_m in Å and ϵ in kcal/mol) for Magnesium, Nitrate, and Acetate

	e	α	R_m	ϵ
O (nitrate)	−0.650	1.200	1.880	0.170
N (nitrate)	+0.950	0.000	1.800	0.160
C (acetate, methyl)	−0.236	0.878	1.908	0.1094
C (acetate, carboxyl)	+0.870	0.616	1.908	0.0860
O (acetate)	−0.835	0.434	1.661	0.2100
H (acetate)	+0.012	0.135	1.487	0.0157
Mg^{2+}	+2.000	0.000	0.923	0.875

Nonbonded interactions were cut off at 12 Å, and long-range electrostatic interactions were accounted for by using the particle mesh Ewald procedure.[30] All bonds involving hydrogen atoms were constrained using the SHAKE algorithm,[31] and a time step of 1 fs was employed. Systems were first equilibrated for 500 ps, after which a 1-ns production run followed, all at 300 K.

A polarizable force field was employed throughout the simulations. To avoid the polarization catastrophe[32] (which can be particularly severe in the presence of multiply charged ions) we have adopted a scheme that introduces a sublinear dependence of the induced dipoles on the electric field above a threshold value of the electric field.[33] As in our previous work, this scaling was chosen such as not to affect the behavior of neat water,[33] for which we employed the POL3 model.[34] For nitrate we have developed a parametrization previously[35] (for better numerical stability we reduced the polarizability by 10%), while for acetate we used the general Amber force field parameter set.[36] For Mg^{2+}, which is missing from this set, we employed the OPLS parameters.[37] Partial charges for acetate and nitrate were evaluated using the standard RESP procedure[38] employing the Gaussian 03 program,[39] and the slab MD simulations were performed using the Amber 8 program.[40] Charges, polarizabilities, and Lennard-Jones parameters for all the studied ions are summarized in Table 1.

The employed force field was verified via comparison of the calculated and experimental ion hydration free energies. For the former we used the free energy preturbation (FEP) method, as implemented in the Gromacs 3.3 program package,[41] for a system of a single ion in a box of 216 water molecules. An NPT ensemble at ambient conditions was employed. Gromacs rather than Amber was used for FEP calculations, since it allows a better control of statistical error of the calculated free energies. The same force field was employed as in the above simulations using the Amber program. Since Gromacs uses Drude oscillators to describe polarization interactions, we have transformed atomic polarizabilities from Amber to the corresponding Drude oscillator parameters. We were able to converge the hydration free energies within a residual relative error of 10%. The calculated (experimental) values are −420 (−433)[42] kcal/mol for Mg^{2+}, −72 (−77)[1] kcal/mol for NO_3^-, and −94 (−80)[43] kcal/mol for Ac^-. Thus, the calculated values within their statistical error match the experiment, except for acetate, where the hydration free energy is slightly overestimated (which means that the present results should provide a lower bound for the surface propensity and ion pairing tendency of acetate).

Experimental Section

$Mg(OAc)_2{\cdot}4H_2O$ (>99%, SRL, India), $Mg(NO_3)_2{\cdot}6H_2O$ (>99%, SD Fine Chemicals, India), and $MgCl_2{\cdot}6H_2O$ (>99%, E Merck, India) were recrystallized twice from double-distilled water and finally dried in a desiccator over P_2O_5 under vacuum. All solutions were prepared using double-distilled water and by successive dilution of a stock solution. The final concentrations were checked by complexometric titration against EDTA.[44]

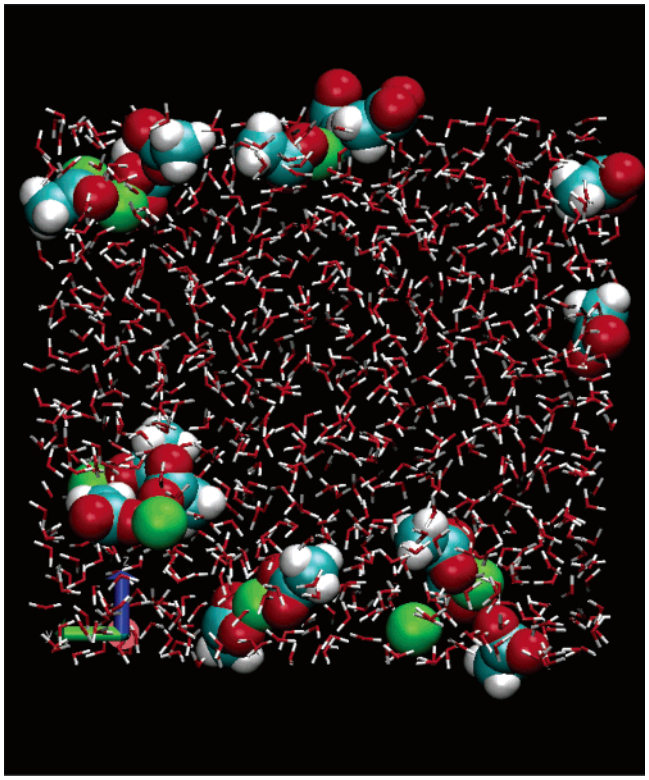

Figure 1. A snapshot from a simulation of a slab of 0.5 M $Mg(OAc)_2$-(aq). Color coding: Mg, green; C, cyan; O, red; H, white. For clarity, water molecules are displayed in the stick representation. Note the surface accumulation of acetate ions (top and bottom).

The surface tension, σ, of all solutions was measured with a dynamic contact angle meter and tentiometer (DCAT-11, DataPhysics, Germany) using a Wilhelmy plate with an accuracy of ± 0.01 mN m^{-1} at 298.15 K. The temperature of the measurements (298.15 K) was controlled by circulating thermostated liquid through from F32HP circulator (Julabo, Germany), and minimum triplicate measurements were made at each concentration, which was varied from 0.0145 to 6.545 M/mol dm^{-3}.

Results and Discussion

Surface propensity and ion pairing was investigated by MD simulations in slab geometry of solutions of magnesium acetate and magnesium nitrate with mean concentrations ranging from 0.5 to 2 M. Figures 1 and 2 depict typical snapshots from simulations of the two systems at 0.5 M. The difference between the two solutions is dramatic. On one hand, $Mg(NO_3)_2$(aq) is at the given concentration a well-behaved, close-to-ideal solution with extensive ion−water mixing and virtually no formation of contact ion pairs. Magnesium dications are strongly repelled from the surface and the only nonclassical[16,17] feature is the weak propensity of nitrate for the solution/vapor interface (top and bottom of Figure 2). On the other hand, the 0.5 M aqueous solution of $Mg(OAc)_2$ is highly nonideal, with strong ion pairing and even clustering (Figure 1). This behavior has been pointed to and analyzed already in our recent study of bulk solutions of magnesium acetate.[14] Also note that ion clustering has recently been observed in another solution containing monovalent organic and divalent inorganic ions, namely aqueous guanidinium sulfate.[13] In addition, we see in our slab simulations a very strong surface propensity for acetate. As a matter of fact,

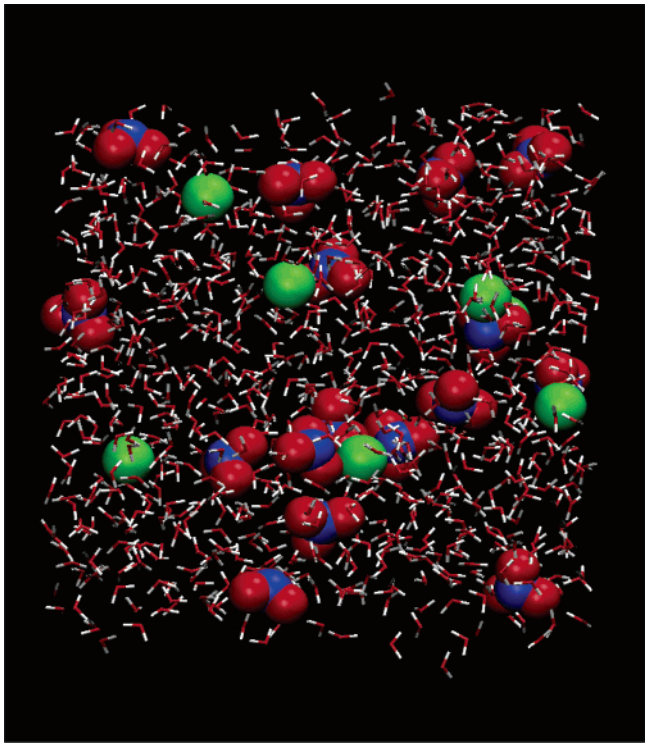

Figure 2. A snapshot from a simulation of a slab of 0.5 M $Mg(NO_3)_2$-(aq). Color coding: Mg, green; N, blue; O, red; H, white.

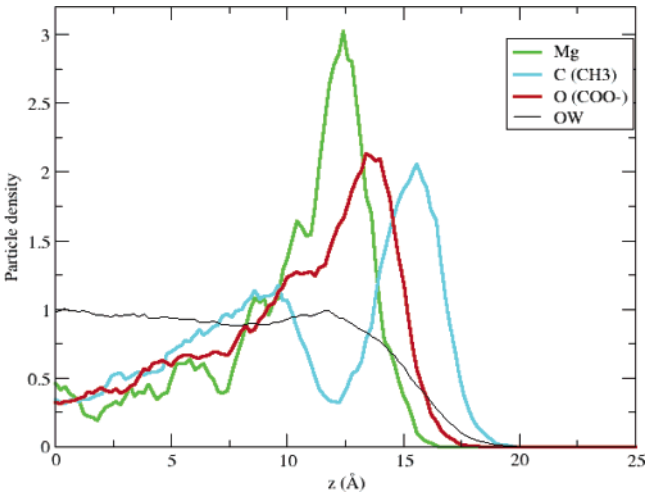

Figure 3. Density profiles (i.e., abundancies of individual species from the center of the slab across the air/solution interface into the gas phase) in a slab of 2 M $Mg(OAc)_2$(aq) solution.

a large fraction of acetate anions segregates at the interfacial layer, into which the anions tend to drag also the magnesium dications (top and bottom of Figure 1).

The difference between the two solutions persists (or even becomes stronger) for higher concentrations. Below we present a quantitative analysis of 2 M solutions of $Mg(OAc)_2$ and $Mg(NO_3)_2$, where the sampling statistics is significantly improved compared to the 0.5 M solutions. Figures 3 and 4 show the density profiles, i.e., abundances of individual species in layers parallel to the surface, from the center of the slab across the solution/vapor interface into the gas phase, for the two solutions. In both cases the bulk aqueous, interfacial, and vapor phases are defined by the water density profile (black line). As in our previous studies,[21] the normalization of the density profiles is such that the value for water density in the center of

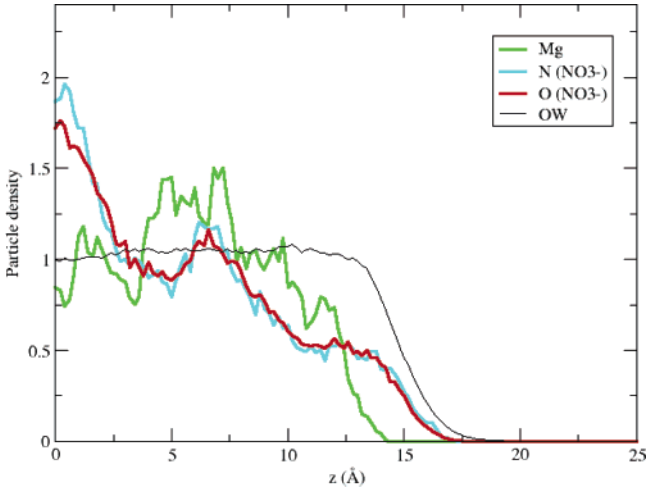

Figure 4. Density profiles in a 2 M $Mg(NO_3)_2$(aq) solution.

the slab is unity and the integral under all the curves is the same. Note that the density profiles are not fully converged in the subsurface/bulk region due to the finite thickness of our slabs. We have shown in our previous work[45,46] that despite this problem (the full remedy of which would require computationally hardly feasible unit cell sizes) the surface propensity is practically converged for the present system size.

Acetate exhibits a sizable surfactant behavior with an interfacial density peak (Figure 3). Its surface affinity is due to two factors: the hydrophobicity of the methyl group and the polarization effect (test MD runs with polarizability turned off show a significantly reduced surface propensity of acetate). Note that the signal from the carbon atom of the methyl group is shifted by about 2 Å toward the vapor phase with respect to that of the acetate oxygens (Figure 3). This clearly indicates a strong orientation of acetate anions in the interfacial layer with the hydrophilic COO^- group being anchored in water and the hydrophobic methyl group pointing into the gas phase. Recently, similar surface orientational ordering has been observed for aqueous dicarboxylate dianions with an aliphatic bridging group.[47] Mg^{2+}ions exhibit a strong subsurface peak shifted by about 1 Å from that of acetate oxygens, creating thus with acetate anions a weak effective interfacial electric double layer (Figure 3). This subsurface peak is the results of two competing forces: the sizable electrostatic repulsion of hard dications from the air/water interface and the surface electroneutrality effect, which becomes rather strong at higher (molar) concentrations.

The density profiles of $Mg(NO_3)_2$(aq) are very different from those of $Mg(OAc)_2$(aq). Nitrate exhibits a weak propensity for the solution/vapor interface and can be occasionally found even in the topmost layer; however, its density profile does not exhibit any surface peak (Figure 4), in accordance with the result of most recent MD simulations of a slab of aqueous sodium nitrate.[48] In our previous study of a single nitrate anion at the air/water interface, we have observed a somewhat stronger surface propensity;[35] however, the present studies have better statistics and also employ a polarizability cutoff scheme,[33] which should slightly reduce the surface ion effect. Since there is no sizable surface enhancement of NO_3^-, the surface electroneutrality force is weak and, consequently, the electrostatic repulsion of Mg^{2+} dominates and the interfacial layer is almost devoid of dications (Figure 4).

We characterized the degree of ion pairing separately in the bulk and interfacial regions of the solutions in terms of dication−anion radial distribution functions (RDF) and the

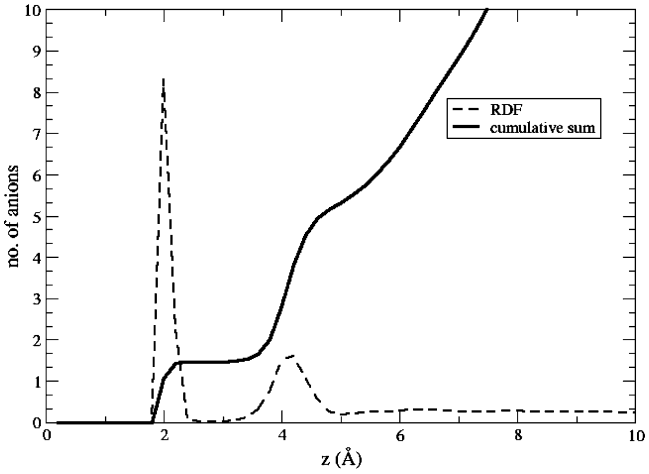

Figure 5. Mg^{2+}−oxygen of acetate ion radial distribution function (RDF) and cumulative sum (i.e., integrated RDF) for the interfacial layer of a slab of 2 M $Mg(OAc)_2$(aq). The normalized RDF is scaled down by a factor of 10, so that the two curves can be shown in a single plot.

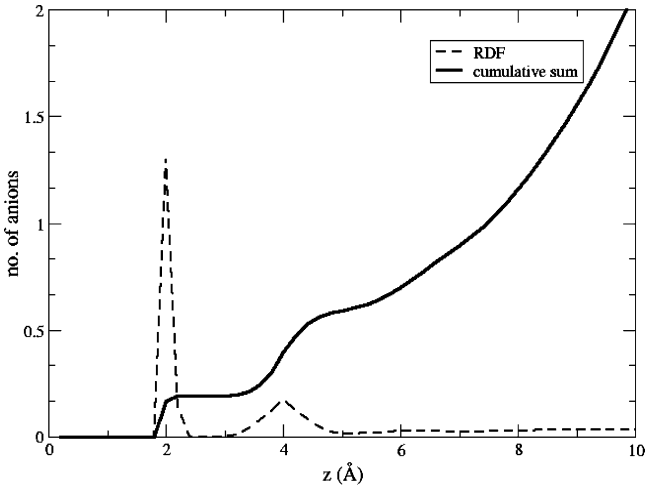

Figure 6. Mg^{2+}−oxygen of acetate ion radial distribution function and cumulative sum for the bulk region of a slab of 2 M $Mg(OAc)_2$(aq). The normalized RDF is scaled down by a factor of 10.

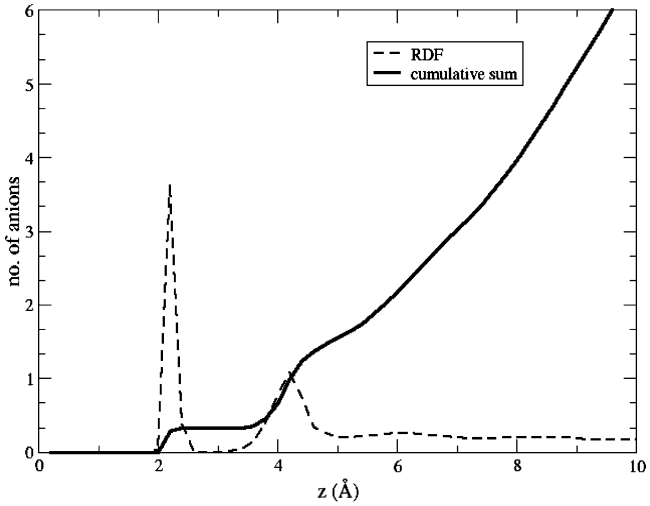

Figure 7. Mg^{2+}−oxygen of nitrate ion radial distribution function and cumulative sum for the interfacial layer of a slab of 2 M $Mg(NO_3)_2$(aq). The normalized RDF is scaled down by a factor of 10.

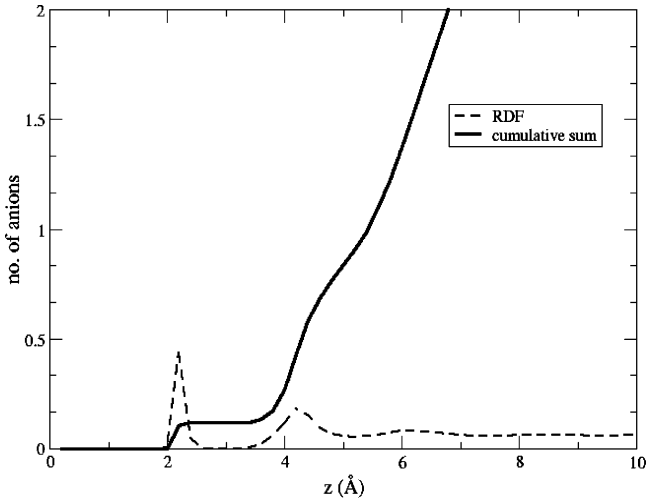

Figure 8. Mg^{2+}−oxygen of nitrate ion radial distribution function and cumulative sum for the bulk region of a slab of 2 M $Mg(NO_3)_2$(aq). The normalized RDF is scaled down by a factor of 10.

corresponding cumulative sums. The latter quantities, which are the integrated values of RDF, give the total number of anions within a certain distance from Mg^{2+}. Figure 5 shows the Mg^{2+}−oxygen of acetate RDF and the cumulative sum for the interfacial layer, while the same quantities for the bulk region are depicted in Figure 6. The strong RDF peak at 2.1 Å corresponds to prevalent formation of contact ion pairs at the interface: on average every magnesium dication is directly paired with ∼1.5 acetate anions (Figure 5). This strong tendency for ion pairing also results in clustering of ions within the interface. A direct consequence of this is the appearance of magnesium-bridged acetate−acetate pairs. The second RDF peak around 4.1 Å correlates with solvent separated ion pairs. The RDF pertinent to the bulk region looks qualitatively similar to the interfacial one; however, the tendency for ion pairing is significantly reduced (Figure 6). This might be partially due to the better ability of bulk water molecules, compared to those at the surface, to dissolve the salt, but the dominant factor is the dramatically reduced ion concentration in the bulk. Due to the surface segregation of the aqueous magnesium acetate, the remaining amount of bulk ions corresponds to a significantly lower concentration than the nominal value of 2 M, while the surface salt concentration strongly exceeds this value. The concentration in the central region of the slab is even smaller than the value of 1 M adopted in our previous bulk study;[14] consequently, the degree of ion pairing (which increases with concentration) is also lower.

The situation is again very different in aqueous magnesium nitrate. Within our previous study of bulk 1 M solution, we did not observe any appreciable ion pairing in $Mg(NO_3)_2$(aq).[14] Here, at 2 M, we see the very onset of formation of contact ion pairs (Figures 7 and 8). More precisely, in the bulk region of the slab there is less than 0.2 nitrate anions directly paired with magnesium. Within the interface this number slightly increases (to about 0.4); however, the statistics is poorer there, due to the smaller amount of ions present.

The vastly different interfacial structures of the two solutions should be also reflected in surface tension trends. Namely, $Mg(NO_3)_2$(aq) behaves as typical inorganic salts, where cations are per se strongly repelled from the surface, while anions exhibit a certain surface propensity (very weak in case of nitrate). As a result, there is a net depletion of ions from the interfacial layer, which translates via the Gibbs adsorption equation into an increase of surface tension compared to neat

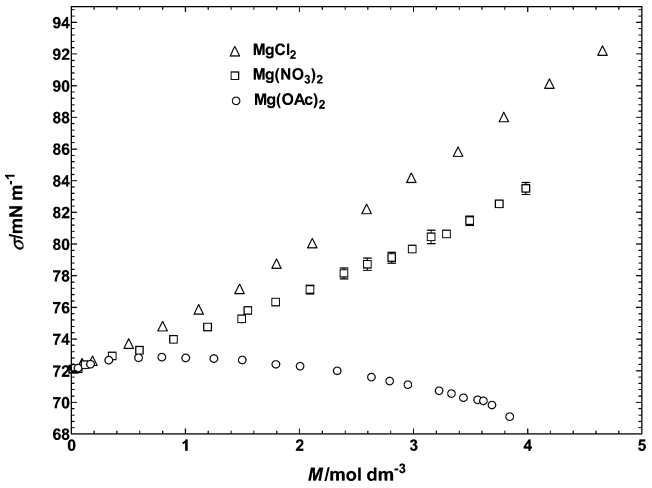

Figure 9. Measured surface tension of $Mg(OAc)_2$(aq), $Mg(NO_3)_2$(aq), and $Mg(Cl)_2$(aq) as a function of salt concentration. Note the decreasing surface tension at higher concentrations in the former case, as opposed to an almost linear surface tension increase in the latter two cases. The error bars indicate the statistical error, which is about 1%.

water.[49,50] This is indeed born out of our MD simulations, where we evaluated surface tension from the trajectory-averaged asymmetry of the pressure tensor.[51]

We have calculated surface tensions for the two salt solutions for different concentrations from 0.5 to 2 M. We should stress that these results suffer both from systematic and statistical errors. The systematic error is primarily due to force field deficiencies (standard force fields give surface tension values of neat water within 60 mN/m from the experimental value).[52] The presently used force field performs acceptably from this point of view, underestimating the surface tension of water by ~17 mN/m.[52] The statistical error is due to finite simulation length and large pressure fluctuations (due to low compresibility of water). Within present simulations the root-mean-square deviations amounts to 1−2 mN/m. In order not to overinterpret the calculated surface tensions suffering from the above inaccuracies, we only provide the conclusions that are beyond the statistical and systematic errors, namely, that upon addition of magnesium acetate the surface tension does not change beyond the statistical error, while upon addition of magnesium nitrate it increases by ~2 mNm^{-1} M^{-1}.

The computational results are supported by surface tension measurements for aqueous magnesium acetate, nitrate, and chloride in a wide range of concentrations. Variations of surface tension of the studied aqueous electrolyte solutions with concentration at 298.15 K are depicted in Figure 9. The measured surface tension values of the three aqueous electrolyte solutions are within ± 0.7% of literature data[53,54] wherever available.

The general behavior of the surface tension isotherms of $Mg(NO_3)_2$(aq) and $MgCl_2$(aq) are similar to each other: in both cases surface tension increases with concentration [more for $MgCl_2$(aq) than $Mg(NO_3)_2$(aq)] like for other inorganic salts.[53] For $Mg(OAc)_2$(aq), however, the surface tension isotherm weakly increases only up to ~0.5 M, after which a monotonic decrease with concentration is observed. The significant differences in surface tension isotherm in these three aqueous electrolyte solutions definitely suggest that the anions play a key role in modifying the surfaces. In the case of $Mg(OAc)_2$(aq), the decrease in the surface tension beyond ~0.5 M envisages the accumulation of CH_3COO^- like that of surfactants (surface active agent) with polar head toward the bulk phase and the hydrophobic group toward the interface, in agreement with the MD results.

Conclusions

Molecular dynamics simulations reveal a very different behavior at the solution/vapor interface of $Mg(OAc)_2$(aq) vs $Mg(NO_3)_2$(aq). As in the aqueous bulk,[14] there is a strong tendency for formation of contact ion pairs and even ion clusters in the former but not in the latter system. Moreover, acetate exhibits a strong surface affinity both due to the hydrophobicity of its methyl group and due to polarization interactions. In contrast, hydrophilic and polarizable nitrate shows only a weak propensity for the solution/vapor interface and the hard magnesium dication is per se strongly repelled from the surface. Due to the accumulation of acetate anions in the interfacial layer, magnesium dications are, however, dragged to the subsurface of $Mg(OAc)_2$(aq) by the surface electroneutrality requirement. This results in a creation of an effective electric double layer and in increased ion pairing and clustering in the interface. The different interfacial structure of aqueous magnesium acetate and magnesium nitrate is also reflected in opposite trends in surface tension change with concentration. Experiments show that the surface tension of $Mg(NO_3)_2$(aq) increases roughly linearly with concentration, similarly as (but less than) for another inorganic magnesium salt, $Mg(Cl)_2$(aq). In $Mg(OAc)_2$(aq), however, the surface tension curve exhibits a crossover around 0.5 M, after which it starts to decrease, indicating net accumulation of ions in the interfacial layer. These experimental findings are directly supported by results from molecular dynamics simulations.

Acknowledgment. S.M. is grateful to the Director, Regional Research Laboratory, Jorhat, India, for interest in this work, and the Department of Science and Technology, New Delhi, India, for partial financial support. Support from the Czech Ministry of Education (grants LC512 and ME644) and from the US-NSF (grants CHE 0431312 and 0209719) is gratefully acknowledged. B.M. would like to thank the Granting Agency of the Czech Republic for support (grant 203/05/H001).

References and Notes

(1) Marcus, Y. *Ion Solvation*; Wiley: Chichester, 1985.
(2) Degreve, L.; da Silva, F. L. B. *J. Chem. Phys.* **1999**, *111*, 5150−5156.
(3) Degreve, L.; da Silva, F. L. B. *J. Chem. Phys.* **1999**, *110*, 3070−3078.
(4) Vieira, D. S.; Degreve, L. *J. Mol. Struct.*—THEOCHEM **2002**, *580*, 127−135.
(5) Degreve, L.; Mazze, F. M. *Mol. Phys.* **2003**, *101*, 1443−1453.
(6) Laudernet, Y.; Cartailler, T.; Turq, P.; Ferrario, M. *J. Phys. Chem. B* **2003**, *107*, 2354−2361.
(7) Harsanyi, I.; Pusztai, L. *J. Chem. Phys.* **2005**, *122*.
(8) Heyrovska, R. *J. Electrochem. Soc.* **1996**, *143*, 1789−1793.
(9) Buchner, R.; Chen, T.; Hefter, G. *J. Phys. Chem. B* **2004**, *108*, 2365−2375.
(10) Chen, T.; Hefter, G.; Buchner, R. *J. Solution Chem.* **2005**, *34*, 1045−1066.
(11) Chialvo, A. A.; Simonson, J. M. *Mol. Phys.* **2002**, *100*, 2307−2315.
(12) Tromans, A.; May, P. M.; Hefter, G.; Sato, T.; Buchner, R. *J. Phys. Chem. B* **2004**, *108*, 13789−13795.
(13) Mason, P. E.; Dempsey, C. E.; Neilson, G. W.; Brady, J. W. *J. Phys. Chem. B* **2005**, *109*, 24185−24196.
(14) Wahab, A.; Mahiuddin, S.; Hefter, G.; Kunz, W.; Minofar, B.; Jungwirth, P. *J. Phys. Chem. B* **2005**, *109*, 24108−24120.
(15) Chorny, I.; Dill, K. A.; Jacobson, M. P. *J. Phys. Chem. B.* **2005**, *109*, 24056−24060.
(16) Onsager, L.; Samaras, N. N. T. *J. Chem. Phys.* **1934**, *2*, 528−536.
(17) Randles, J. E. B. *Phys. Chem. Liq.* **1977**, *7*, 107.
(18) Jungwirth, P.; Tobias, D. J. *J. Phys. Chem. B* **2001**, *105*, 10468−10472.

(19) Dang, L. X.; Chang, T. M. *J. Phys. Chem. B* **2002**, *106*, 235−238.
(20) Dang, L. X. *J. Phys. Chem. B* **2002**, *106*, 10388−10394.
(21) Jungwirth, P.; Tobias, D. J. *J. Phys. Chem. B* **2002**, *106*, 6361−6373.
(22) Archontis, G.; Leontidis, E.; Andreou, G. *J. Phys. Chem. B* **2005**, *109*, 17957−17966.
(23) Ghosal, S.; Hemminger, J. C.; Bluhm, H.; Mun, B. S.; Hebenstreit, E. L. D.; Ketteler, G.; Ogletree, D. F.; Requejo, F. G.; Salmeron, M. *Science* **2005**, *307*, 563−566.
(24) Petersen, P. B.; Saykally, R. J. *Chem. Phys. Lett.* **2004**, *397*, 51−55.
(25) Petersen, P. B.; Johnson, J. C.; Knutsen, K. P.; Saykally, R. J. *Chem. Phys. Lett.* **2004**, *397*, 46−50.
(26) Liu, D. F.; Ma, G.; Levering, L. M.; Allen, H. C. *J. Phys. Chem. B* **2004**, *108*, 2252−2260.
(27) Benjamin, I. *J. Chem. Phys.* **1991**, *95*, 3698−3709.
(28) Wilson, M. A.; Pohorille, A. *J. Chem. Phys.* **1991**, *95*, 6005−6013.
(29) Allen, M. P.; Tildesley, D. J. *Computer Simulations of Liqiuds*; Clarendon: Oxford, 1987.
(30) Essmann, U.; Perera, L.; Berkowitz, M. L.; Darden, T.; Lee, H.; Pedersen, L. G. *J. Chem. Phys.* **1995**, *103*, 8577−8593.
(31) Ryckaert, J.-P.; Ciccotti, G.; Berendsen, H. J. C. *J. Comput. Phys.* **1977**, *23*, 327−341.
(32) Thole, B. T. *Chem. Phys.* **1981**, *59*, 341−350.
(33) Petersen, P. B.; Saykally, R. J.; Mucha, M.; Jungwirth, P. *J. Phys. Chem. B* **2005**, *109*, 10915−10921.
(34) Caldwell, J. W.; Kollman, P. A. *J. Phys. Chem.* **1995**, *99*, 6208−6219.
(35) Salvador, P.; Curtis, J. E.; Tobias, D. J.; Jungwirth, P. *Phys. Chem. Chem. Phys.* **2003**, *5*, 3752−3757.
(36) Wang, J. M.; Wolf, R. M.; Caldwell, J. W.; Kollman, P. A.; Case, D. A. *J. Comput. Chem.* **2004**, *25*, 1157−1174.
(37) Jorgensen, W. L. *OPLS and OPLS-AA Parameters for Organic Molecules, Ions, and Nucleic Acids*; Yale University: New Haven, CT, 1997.
(38) Bayly, C. I.; Cieplak, P.; Cornell, W. D.; Kollman, P. A. *J. Phys. Chem.* **1993**, *97*, 10269−10280.
(39) Frisch, M. J. T., G. W.; Schlegel, H. B.; Scuseria, G. E.; Robb, M. A.; Cheeseman, J. R.; Montgomery, J. A., Jr.; Vreven, T.; Kudin, K. N.; Burant, J. C.; Millam, J. M.; Iyengar, S. S.; Tomasi, J.; Barone, V.; Mennucci, B.; Cossi, M.; Scalmani, G.; Rega, N.; Petersson, G. A.; Nakatsuji, H.; Hada, M.; Ehara, M.; Toyota, K.; Fukuda, R.; Hasegawa, J.; Ishida, M.; Nakajima, T.; Honda, Y.; Kitao, O.; Nakai, H.; Klene, H.; Li, X.; Knox, J. E.; Hratchian, H. P.; Cross, J. B.; Adamo, C.; Jaramillo, J.; Gomperts, R.; Stratmann, R. E.; Yazyev, O.; Austin, A. J.; Cammi, R.; Pomelli, C.; Ochterski, J. W.; Ayala, P. Y.; Morokuma, K.; Voth, G. A.; Salvador, P.; Dannenberg, J. J.; Zakrzewski, V. G.; Dapprich, S.; Daniels, A. D.; Strain, M. C.; Farkas, O.; Malick, D. K.; Rabuck, A. D.; Raghavachari, K.; Foresman, K. J.; Ortiz, J. V.; Cui, Q.; Baboul, A. G.; Clifford, S.; Cioslowski, J.; Stefanov, B. B.; Liu, G.; Liashenko, A.; Piskorz, P.; Komaromi, I.; Martin, R. L.; Fox, D. J.; Keith, T.; Al-Laham, M. A.; Peng, C. Y.; Nanayakkara, A.; Challacombe, M.; Gill, P. M. W.; Johnson, B.; Chen, W.; Wong, M. W.; Gonzalez, C.; Pople, J. A. *Gaussian 03:* Gaussian: Pittsburgh, PA, 2003.
(40) Case, D. A. D., T. A.; Cheatham, III, T. E.; Simmerling, C. L.; Wang, J.; Duke, R. E.; Luo, R.; Merz, K. M.; Wang, B.; Pearlman, D. A.; Crowley, M.; Brozell, S.; Tsui, V.; Gohlke, H.; Mongan, J.; Hornak, V.; Cui, G.; Beroza, P.; Schafmeister, C.; Caldwell, J. W.; Ross, W. S.; Kollman, P. A. *Amber 8;* University of California: San Francisco, 2004.
(41) Lindahl, E.; Hess, B.; van der Spoel, D. *J. Mol. Model.* **2001**, *7*, 306−317.
(42) Schmid, R.; Miah, A. M.; Sapunov, V. N. *Phys. Chem. Chem. Phys.* **2000**, *2*, 97−102.
(43) Kelly, C. P.; Cramer, C. J.; Truhlar, D. G. *J. Chem. Theory Comput.* **2005**, *1*, 1133−1152.
(44) Vogel, A. I. *Textbook of Quantitative Inorganic Analysis*; Longman: London, 1985.
(45) Vrbka, L.; Mucha, M.; Minofar, B.; Jungwirth, P.; Brown, E. C.; Tobias, D. J. *Curr. Opin. Colloid Interface Sci.* **2004**, *9*, 67−73.
(46) Jungwirth, P.; Tobias, D. J. *Chem. Rev.* **2006**, *106*, 1259−1281.
(47) Minofar, B.; Mucha, M.; Jungwirth, P.; Yang, X.; Fu, Y. J.; Wang, X. B.; Wang, L. S. *J. Am. Chem. Soc.* **2004**, *126*, 11691−11698.
(48) Dang, L. X.; Chang, T. M.; Roeselova, M.; Garrett, B. C.; Tobias, D. J. *J. Chem. Phys.* **2006**, *124*, 066101.
(49) Gibbs, J. W. *The Collected Works of J. Willard Gibbs*; Longmans: New York, 1928.
(50) Defay, R.; Prigogine, I.; Bellemans, A. *Surface Tension and Adsorption*; Longmans Green: London, 1966.
(51) Zhang, Y. H.; Feller, S. E.; Brooks, B. R.; Pastor, R. W. *J. Chem. Phys.* **1995**, *103*, 10252−10266.
(52) Garrett, B. C.; Schenter, G. K.; Morita, A. *Chem. Rev.* **2006**, *106*, 1355−1374.
(53) *International Critical Tables*; Washburn, E. W., Ed.; McGraw-Hill: New York, 1928; Vol. 4.
(54) Weissenborn, P. K.; Pugh, R. J. *J. Colloid Interface Sci.* **1996**, *184*, 550−563.